Analysis of Fluorescence Spectra of Rare-earth Chelates. Part IV.[1-3] Effects of *para*-Bromo-substitution on Internal Stark Splitting and Molecular Geometry of Tetrakis(dibenzoylmethido)europate(III)

By **John J. Degnan, Charles R. Hurt, and Nicolae Filipescu,*** NASA, Goddard Space Flight Center, Greenbelt Maryland 20771 and Department of Chemistry, The George Washington University, Washington, D.C. 20006

The fluorescence spectrum of tetraethylammonium tetrakis(di-*p*-bromodibenzoylmethido)europate(III) was analysed in detail by treating the ligand field as a perturbation on the free-ion levels. From the splitting in the $^7F_1$ and $^7F_2$ levels of Eu^{3+} ion the ligand-field parameters were calculated without assuming a known molecular geometry and the structure suggested by these parameters is discussed. Comparison of parameter values of the *p*-bromo-substituted chelate with those of the unsubstituted dibenzoylmethide indicates that a substantial change in molecular geometry has occurred on replacing the *para*-H atoms with Br. Further, the experimentally derived parameters allowed calculation of interatomic distances and bond angles and suggested an increase in charge density in the vicinity of the lanthanide ion on *p*-bromo-substitution.

In previous Parts [1-3] we explained the splitting pattern observed in the fluorescence spectra of octaco-ordinated β-ketoenolates of Eu^{3+} by treating the ligand field as a perturbation on the free-ion levels. The ligand-field parameters were calculated from the splitting in the $^7F_1$ and $^7F_2$ levels without assuming a known molecular geometry. The values of the parameters derived from the fluorescence spectra established the geometry of tetrakis(dibenzoylmethido)europate(III) anion,[1] the influence of the organic cation,[3] and the structure of two mixed bipyridyl complexes of europic chloride.[2] In addition, the ligand-field parameters were used to calculate interatomic distances and bond angles.

We now report the effect of *para*-bromo-substitution on the splitting pattern and molecular geometry of tetraethylammonium tetrakis(dibenzoylmethido)europate(III) (EuD_4T). As previously demonstrated, the tetraethylammonium ion does not significantly influence the geometry of the octaco-ordinated anion because of its considerable steric hindrance.[1,3] It is interesting that the *para*-substituted bromine atoms change not only the charge on the complexing oxygen atoms through resonance and inductive effects but also determine a radical change in geometry from the configuration of the unsubstituted chelate. This is reflected in the Stark splitting of the Eu^{3+} levels and is confirmed by the values of the ligand-field parameters determined from the fluorescence spectrum.

EXPERIMENTAL

*Preparation of Tetraethylammonium Tetrakis(di-*p*-bromodibenzoylmethido)europate*(III) $Eu(BD)_4T$.—*Synthesis of ligand.* 4,4′-Dibromodibenzoylmethane was prepared from ethyl *p*-bromobenzoate and *p*-bromoacetophenone (Aldrich Organic Chemicals) by the condensation procedure described by Harris and Levine,[4] method A. The ester was synthesised from *p*-bromobenzoyl chloride (Eastman) and ethanol.

Preparation of chelate. To a mechanically stirred hot solution of β-diketone ligand (0·382 g; 1 mmol) and aqueous 10% tetraethylammonium hydroxide (Eastman) (1·4 ml) in ethanol (25 ml), anhydrous europium chloride (American Potash, Lindsey) (0·065 g; 0·25 mmol) in ethanol (25 ml) was added slowly. The solution was filtered hot and left overnight. The *crystals* were collected, washed several times with hot 95% ethanol, air-dried, and placed in a desiccator over silica gel. They had m.p. 233—235 °C (decomp.) (Found: C, 44·9; H, 2·9; Br, 34·6; N, 0·85; Eu, 9·3. $C_{68}H_{56}Br_8EuNO_8$ requires C, 45·2; H, 3·1; Br, 35·4; N, 0·78; Eu, 8·43%).

Fluorescence Spectra.—The experimental set-up and procedure for the recording of high-resolution fluorescence spectra of polycrystalline chelate at liquid-nitrogen temperature with the Cary model 14 spectrophotometer were described.[1-3]

Ligand-field Parameters.—Our method of calculation [1] of ligand-field parameters from experimental fluorescence data is based on operator-equivalent procedure developed by Stevens [5] and Judd.[6] The values of the parameters, however, are not obtained theoretically from an assumed molecular model but are extracted from spectral data.

Solution of secular determinants for the $^7F_1$ and $^7F_2$ levels of an Eu^{3+} ion incorporated in a chelate molecule having at least one two-fold axis of symmetry gives respectively the expressions [1] (1) and (2), where X is given by

$$E_1 = E_0 - 2\alpha_1\langle r^2\rangle\beta_2^0 \quad (1a)$$

$$E_2 = E_0 + \alpha_1\langle r^2\rangle\beta_2^0 + \alpha_1\langle r^2\rangle\beta_2^2 \quad (1b)$$

$$E_3 = E_0 + \alpha_1\langle r^2\rangle\beta_2^0 - \alpha_1\langle r^2\rangle\beta_2^2 \quad (1c)$$

$$E_1 = E_0 + 6\alpha_2\langle r^2\rangle\beta_2^0 + 12\beta_2\langle r^4\rangle\beta_4^0 - 12\beta_2\langle r^4\rangle\beta_4^4 \quad (2a)$$

$$E_2 = E_0 - 3\alpha_2\langle r^2\rangle\beta_2^0 - 48\beta_2\langle r^4\rangle\beta_4^0 - 3\alpha_2\langle r^2\rangle\beta_2^2 + 12\beta_2\langle r^4\rangle\beta_4^2 \quad (2b)$$

$$E_3 = E_0 - 3\alpha_2\langle r^2\rangle\beta_2^0 - 48\beta_2\langle r^4\rangle\beta_4^0 + 3\alpha_2\langle r^2\rangle\beta_2^2 - 12\beta_2\langle r^4\rangle\beta_4^2 \quad (2c)$$

$$E_{4,5} = E_0 + \frac{84\beta_2\langle r^4\rangle\beta_4^0 + 12\beta_2\langle r^4\rangle\beta_4^4 \pm X}{2} \quad (2d,e)$$

expression (3). In these expressions, $\langle r^l\rangle\beta_l^m$ are the

$$X = [(84\beta_2\langle r^4\rangle\beta_4^0 + 12\beta_2\langle r^4\rangle\beta_4^4)^2 - 24(-\alpha_2\langle r^2\rangle\beta_2^0 + 12\beta_2\langle r^4\rangle\beta_4^0) \cdot (6\alpha_2\langle r^2\rangle\beta_2^0 + 12\beta_2\langle r^4\rangle\beta_4^0 + 12\beta_2\langle r^4\rangle\beta_4^4) + 48(\alpha_2\langle r^2\rangle\beta_2^2 + 3\beta_2\langle r^4\rangle\beta_4^2)^2]^{\frac{1}{2}} \quad (3)$$

[1] Part I, S. Bjorklund, N. Filipescu, N. McAvoy, and J. J. Degnan, *J. Phys. Chem.*, 1968, **72**, 970.
[2] Part II, N. Filipescu, S. Bjorklund, N. McAvoy, and J. J. Degnan, *J. Chem. Phys.*, 1968, **48**, 2895.
[3] Part III, N. Filipescu, J. J. Degnan, and N. McAvoy, *J. Chem. Soc.* (*A*), 1968, 1594.
[4] S. R. Harris and R. Levine, *J. Org. Chem.*, 1948, **70**, 3360.
[5] K. W. Stevens, *Proc. Phys. Soc.*, 1952, *A*, **65**, 209.
[6] B. R. Judd, *Mol. Phys.*, 1959, **2**, 407.

ligand-field parameters, $\alpha_0 = \beta_0 = 0$; $\alpha_1 = -\frac{1}{5}$; $\beta_2 = -\frac{2}{189}$; $\alpha_2 = -\frac{11}{315}$ as given by Judd,[6,7] and E_0 is the average energy of the Stark components within the appropriate J level.

The energy levels in $^7F_2$ obtained from the fluorescence spectra were fed into a computer which tested all possible assignments of the levels to the secular equations (2). Since $\langle r^2\rangle\beta_2^0$ and $\langle r^4\rangle\beta_4^0$ are known from the splitting of the $^7F_1$ level, the remaining four parameters $\langle r^4\rangle\beta_4^0$, $\langle r^4\rangle\beta_4^2$, $\langle r^4\rangle\beta_4^4$, and E_0 are the unknowns in the five equations (2). But $E_4 - E_5 = X$ with the expression for X given by equation (3). For each assignment of different experimental energy values to the levels given by equations (2), a set of values is obtained for each of the four parameters mentioned above. For each of these sets of parameter values, a value for X is computed by use of equation (3). The value X is then chosen which gives the best agreement with the experimental value of $E_4 - E_5$. In this way, the parameters $\langle r^l\rangle\beta_l^m$ and a unique assignment of the energy levels are obtained. The parameter values have thus been obtained for $Eu(BD)_4T$. The observed energy levels have also been compared with those calculated by substituting the derived parameters in equations (1) and (2). The agreement is excellent.

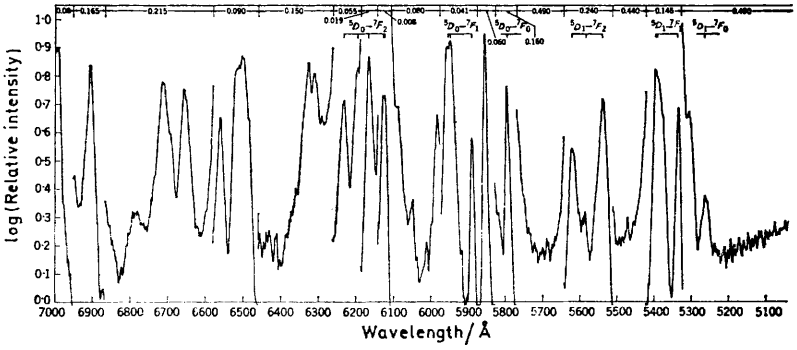

FIGURE 1 Fluorescence spectrum of tetrakis(dibenzoylmethido)europate(III). Slit widths (mm) are given at the top

DISCUSSION

Examination of the fluorescence spectrum shown in Figure 1 reveals the presence of two main Stark components in the $^5D_0 \longrightarrow {}^7F_1$ region (5850—5950 Å), one of which is split by 19 cm^{-1}. In the $^5D_0 \longrightarrow {}^7F_2$ region (6100—6250 Å) one can distinguish four principal lines, one of which is a doublet with a 12 cm^{-1} splitting. By contrast the emission spectrum of microcrystalline EuD_4T exhibited only three main $^5D_0 \longrightarrow {}^7F_2$ lines two of which were very finely split. Since the splitting in the $^7F_1$ and $^7F_2$ levels of Eu^{3+} ion is a very sensitive test for the geometry of the chelate molecule, we are able to show that in the *p*-bromo-substituted dibenzoylmethide the antiprismatic configuration (III) established for the unsubstituted complex [1] has changed to that of antiprism (IV) (see Figure 2). It can be shown from equations (2) that the basically four-level pattern in $^7F_2$ indicates a significant contribution to the splitting by the $\langle r^4\rangle\beta_4^4$ parameter.[8] This is confirmed by the computer analysis which also indicated that the fine splitting between the nearly degenerate sublevels in $^7F_1$ and $^7F_2$ is due to small contributions from the $\langle r^2\rangle\beta_2^2$ and $\langle r^4\rangle\beta_4^2$ parameters.

Using the concept of equivalent point charges,[1] we find that the ratio of the parameters $\langle r^4\rangle\beta_4^4$ and $\langle r^4\rangle\beta_4^0$ is given by (4), where we have implicitly assumed that

$$\frac{\langle r^4\rangle\beta_4^4}{\langle r^4\rangle\beta_4^0} = \frac{35\sum_{i=1}^{8}\sin^4\theta\cos 4\phi_i}{\sum_{i=1}^{8}35\cos^4\theta_i - 30\cos^2\theta_i + 3} \qquad (4)$$

all eight of the nearest-neighbour oxygens are equivalent. On the basis of the internal symmetry of the chelate ring alone, this is a valid assumption. However, it has been demonstrated [1] that this assumption leads to the conclusion that, in the case of antiprism (III), the parameter $\langle r^4\rangle\beta_4^4$ is zero. This is true regardless of the values for θ and α in Figure 3. The assumption is not strictly valid, however, since a slight inequivalency exists among the oxygens as a result of the D_2 symmetry. As is evident from Figure 3, there are two sets, each

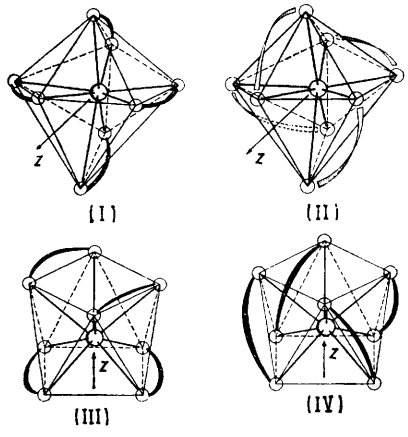

FIGURE 2 Molecular models of dodecahedrons (I) and (II); antiprisms (III) and (IV)

[7] B. R. Judd, *Proc. Roy. Soc.*, 1955, *A*, **228**, 120.
[8] A. Lempicki, H. Samelson, and C. Brecher, *J. Mol. Spectroscopy*, 1968, **27**, 375.

containing four equivalent oxygens. The oxygens within a given set contribute equally to the $\langle r^4\rangle\beta_4^4$ parameter, but the two sets contribute oppositely in sign. Thus the $\langle r^4\rangle\beta_4^4$ parameter can take on substantial non-zero values for antiprism (III) only if the asymmetry in the chelate-charge distribution (resulting from non-symmetric ligand–ligand repulsions) is exceptionally pronounced. It can be shown that, in order to achieve a parameter value equal in magnitude to the one reported here, *ca.* 90% of the total ligand charge would be contained in one-half of the ligand. Alternatively, the differences between the radial distances to inequivalent oxygen sites from the europium ion would be *ca.* 20% or 0·5 Å. Neither of these conclusions is supported by available *X*-ray diffraction data for compounds having the molecular configuration of antiprism (III).[9] The latter studies show the oxygens to be essentially equivalent with respect to charge concentration and radial distance from the central ion. We therefore reject antiprism (III) as a possible configuration for the present compound.

Specializing equation (4) to the three remaining models (see Figure 3) we obtain equation (5) for (I), equation (6) for (II), and equation (7) for (III).* In

$$\frac{\langle r^4\rangle\beta_4^4}{\langle r^4\rangle\beta_4^0} = \frac{-35\,(\sin^4\theta_1 + \sin^4\theta_2)}{(35\cos^4\theta_1 - 30\cos^2\theta_1 + 3) + (35\cos^4\theta_2 - 30\cos^2\theta_2 + 3)} \quad (5)$$

$$\frac{\langle r^4\rangle\beta_4^4}{\langle r^4\rangle\beta_4^0} = \frac{-35\,(\sin^4\theta_1\cos 4\alpha + \sin^4\theta_2\cos 4\beta)}{(35\cos^4\theta_1 - 30\cos^2\theta_1 + 3) + (35\cos^4\theta_2 - 30\cos^2\theta_2 + 3)} \quad (6)$$

$$\frac{\langle r^4\rangle\beta_4^4}{\langle r^4\rangle\beta_4^0} = \frac{-35\sin^4\theta\sin 4\alpha}{35\cos^4\theta - 30\cos^2\theta + 3} \quad (7)$$

Figure 4 we have plotted the expressions $(3\cos^2\theta_1 - 1) + (3\cos^2\theta_2 - 1) = 0$ and $(35\cos^4\theta_1 - 30\cos^2\theta_1 + 3) + (35\cos^4\theta_2 - 30\cos^2\theta_2 + 3) = 0$ in a θ_1 against θ_2 diagram. These expressions represent the angular dependence in the $\langle r^2\rangle\beta_2^0$ and $\langle r^4\rangle\beta_4^0$ parameters respectively. The first equation gives curve 1 whereas the second yields curves 2 and 3. These curves divide the $[\theta_1,\theta_2]$ plane into separate zones corresponding to different combinations of signs on the $\langle r^2\rangle\beta_2^0$ and $\langle r^4\rangle\beta_4^0$ parameters. For a ligand field generated by negatively charged particles, we obtain the signs shown on the graph. We have shaded the region corresponding to negative signs on both parameters as derived from experimental splittings. The actual molecular geometry generating the ligand field should be represented by a point in this region of the graph. On the same diagram we have indicated the expected locations of the dodecahedra and antiprisms derived theoretically by Kepert for octaco-ordination using the hard-sphere and

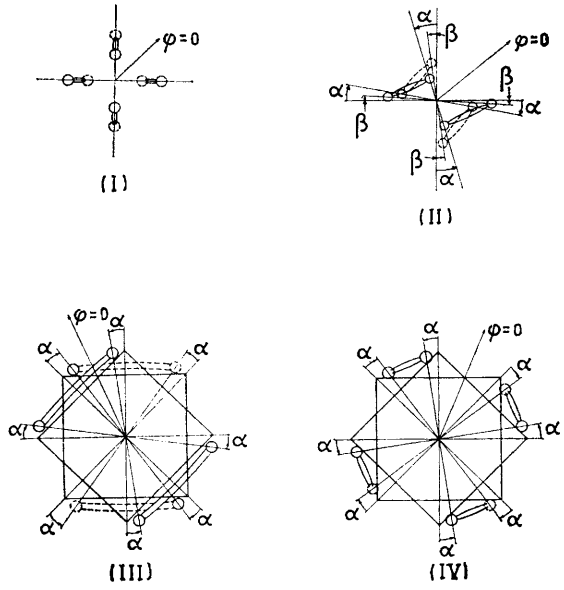

FIGURE 3 Projections of the four models on to the x,y plane showing the choices for the $\phi = 0$ axis and the types of distortion being considered in the present analysis

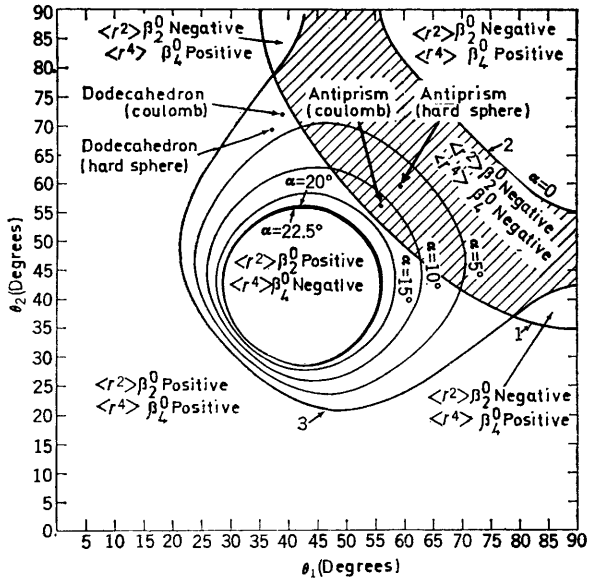

FIGURE 4 Separation of the $[\theta_1,\theta_2]$ plane into regions based on the expected signs of the ligand-field parameters for a molecular Stark field produced by an even number of identical negatively charged particles equally divided into subsets having polar angles θ_1 (or $\pi - \theta_1$) and θ_2 (or $\pi - \theta_2$). Also included is a plot of equation (8) for several values of α using the experimentally derived values of $\langle r^4\rangle\beta_4^4$ and $\langle r^4\rangle\beta_4^0$

coulomb-interaction models.[10] The dodecahedral configurations fall outside the shaded zone in Figure 4. Although this might be sufficient to rule out the dodeca-

* Since the angular part of all ligand-field parameters used in our analysis contains only even powers of sin θ or cos θ, we replaced angles $\theta > \frac{\pi}{2}$ by $\pi - \theta$ for convenience.

[9] B. Matkovic and D. Grdenec, *Acta Cryst.*, 1963, **16**, 456; *Nature*, 1958, **182**, 465.

[10] D. L. Kepert, *J. Chem. Soc.*, 1965, 4736.

hedral geometries as models for the $Eu(BD)_4^-$ anion we will consider the possibility that substantial distortions from the hard-sphere or coulomb model may somehow bring the actual field geometry into the shaded region. For this purpose we find it convenient to plot a 'common' parameter-ratio expression (8) on the θ_1–θ_2 diagram for

$$\frac{\langle r^4\rangle\beta_4^4}{\langle r^4\rangle\beta_4^0} = \frac{-35\,(\sin^4\theta_1 + \sin^4\theta_2)\sin 4\alpha}{(35\cos^4\theta_1 - 30\cos^2\theta_1 + 3) + (35\cos^4\theta_2 - 30\cos^2\theta_2 + 3)} \quad (8)$$

several values of the angle α between 0 and 22·5°. In addition to curves 2 and 3, for which $\alpha = 0$, equation (8) yields five closed loops corresponding to the arbitrary values $\alpha = 5$, 10, 15, 20, and 22·5° respectively (see Figure 4).

If $\sin 4\alpha$ in equation (8) is equal to unity ($\alpha = 22{\cdot}5°$) the resulting expression is identical to equation (5) derived for dodecahedron (I). If the actual ligand field had the geometry of dodecahedron (I), the only combination of θ_1 and θ_2 consistent with the experimental ratio $\langle r^4\rangle\beta_4^4/\langle r^4\rangle\beta_4^0$ are confined to the rim of the inner loop in Figure 4. This loop is not only greatly displaced from the expected values of θ_1 and θ_2 indicated on the same graph, but also lies entirely outside the shaded region. Consequently dodecahedron (I) must be ruled out.

For dodecahedron (II) the angles α and β in equation (6) represent distortions in the ϕ angles from the ideal (undistorted) dodecahedron. For small α and β, equation (6) approaches equation (5). Therefore, in this limit dodecahedron (II) can be rejected on the same grounds as dodecahedron (I). It can be shown that to approach θ angles typical of a dodecahedron and still be consistent with observed ligand-field parameters one needs distortions in the angle ϕ in excess of 18°. This is highly unlikely for two important reasons. First, distortion of the ϕ angles to any great extent would result in large values for the $\langle r^2\rangle\beta_2^2$ and $\langle r^4\rangle\beta_4^2$ parameters contradicting the experimentally observed rather fine splitting caused by these parameters. Secondly, in the undistorted dodecahedra, the ligand 'bite' would find a natural O–Eu–O bond angle of *ca.* 72°. This angle was determined from *X*-ray diffraction patterns in octaco-ordinated ceric acetylacetonate [9] and remained the same for EuD_4T. To satisfy the $\langle r^4\rangle\beta_4^4 : \langle r^4\rangle\beta_4^0$ ratio and approach θ_1 and θ_2 values typical of a dodecahedron, one must visualize distortions which would cause unacceptable bond-bending in the anion bridges and in the O–Eu–O bond angle.

In contrast to the models just discussed, antiprism (IV) allows reasonable agreement between observed spectral splittings and expected bond angles and distances in the chelate molecule. If in equation (8) $\theta_1 = \theta_2 = \theta$ we obtain equation (7) derived for antiprism (IV). Consequently, by looking along the diagonal in Figure 4 ($\theta_1 = \theta_2$) we see that the angle α in antiprism (IV) is confined to the range 0—13°, since larger angles would force us to leave the shaded portion of the graph. Further, on the basis of the large $\langle r^4\rangle\beta_4^4$ parameter we would expect the angle α to be substantial since, as α approaches zero, the parameter $\langle r^4\rangle\beta_4^4$ also approaches zero. Solving for α in equation (7) we find equation (9). Therefore α can be written as a function

$$\alpha = \frac{1}{4}\sin^{-1}\left[-\frac{\langle r^4\rangle\beta_4^4}{\langle r^4\rangle\beta_4^0}\frac{(35\cos^4\theta - 30\cos^2\theta + 3)}{35\sin^4\theta}\right] \quad (9)$$

of θ and $\langle r^4\rangle\beta_4^4/\langle r^4\rangle\beta_4^0$. Further one can show that, for antiprism (IV), the bond angle γ between the europium ion and the two oxygens in a chelate ring is given by the expression (10).

$$\gamma = \cos^{-1}\left[\frac{\sqrt{2}}{2}\sin^2\theta\,(\cos 2\alpha + \sin 2\alpha) - \cos^2\theta\right] \quad (10)$$

The distance between the two oxygen atoms in a ketoenolate ring is taken [9] to be 2·81 Å. This distance does not change significantly upon changing the complexed ion.[11,12] If we now assume that the equivalent point charge lies along the Eu–O bond [1] we obtain expression (11) for the distance between the europium ion and an oxygen atom. Using equations (8), (9), and

$$R_{Eu-O}(\gamma) = \frac{2{\cdot}81}{2\sin\frac{\gamma}{2}} \quad (11)$$

(10) we see that R_{Eu-O} can be expressed as a function of θ and experimental parameters $\langle r^4\rangle\beta_4^4$ and $\langle r^4\rangle\beta_4^0$.

For antiprism (IV) we also have the relationship (12)

$$\frac{\langle r^2\rangle\beta_2^0}{\langle r^4\rangle\beta_4^0} = \frac{16R^2\,(3\cos^2\theta - 1)}{(35\cos^4\theta - 30\cos^2\theta + 3)}\frac{\langle r^2\rangle}{\langle r^4\rangle} \quad (12)$$

between the parameters $\langle r^2\rangle\beta_2^0$ and $\langle r^4\rangle\beta_4^0$, where R is the distance to an equivalent point charge. Solving for R, we obtain equation (13). Setting $\langle r^4\rangle$ and $\langle r^2\rangle$

$$R = \left[\frac{\langle r^2\rangle\beta_2^0}{\langle r^4\rangle\beta_4^0}\frac{(35\cos^4\theta - 30\cos^2\theta + 3)}{16\,(3\cos^2\theta - 1)}\frac{\langle r^4\rangle}{\langle r^2\rangle}\right]^{\frac{1}{2}} \quad (13)$$

equal to $1{\cdot}706a_0^4$ and $0{\cdot}834a_0^2$ respectively (obtained from interpolation of data reported by Freeman and Watson [13]) we obtain an expression for R in terms of θ and the experimental parameters $\langle r^2\rangle\beta_2^0$ and $\langle r^4\rangle\beta_4^0$.

If it is assumed that the equivalent point charges coincide with the positions of the oxygen atoms, the intercept in Figure 5 should give the Eu–O distances and the angle θ. The values obtained are $R = 2{\cdot}40$ Å and $\theta = 55{\cdot}4°$. Substitution of this value of θ into equation (8) along with the experimentally derived ligand-field parameters gives an angle $\alpha = 12{\cdot}2°$. From equation (10), the O–Eu–O bond angle is then found to be 71·8°.

[11] G. T. Bullen, R. Mason, and P. Pauling, *Nature*, 1961, **189**, 291.

[12] The constancy of the 'ligand bite' was also used by W. G. Perkins and G. A. Crosby, *J. Chem. Phys.*, 1965, **42**, 407, 2621 in crystal-field calculations on Yb^{3+} and Tm^{3+} tris β-keto-enol complexes.

[13] A. J. Freeman and R. E. Watson, *Phys. Rev.*, 1962, **127**, 2058.

Both the Eu–O distance and O–Eu–O bond angle agree with that found for the unsubstituted chelate [1] which was believed to have the geometry of antiprism (III).

It should be pointed out that the essential features of the Stark splittings observed for the unsubstituted chelate can be adequately described in terms of the

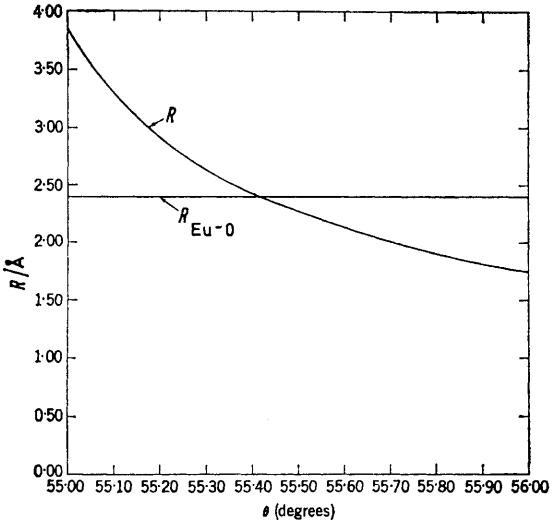

FIGURE 5 Plot of R_{Eu-O} and R versus the polar angle θ. The intercept of the two curves gives the radial distance to the oxygen atom and the polar angle

diagonal elements in the secular determinants for $^7F_1$ and $^7F_2$ with only relatively minor contribution from the off-diagonal elements.[1] This suggests that in this chelate the europium ion sees a ligand field approaching a unidentate antiprismatic D_{4d} symmetry even though the total symmetry of model (III) is D_2. This further implies that, by comparison with the nearest-neighbour oxygen, the rest of the chelate rings contribute little to the ligand field. By contrast, in the dibromo-substituted chelate, the Stark splitting cannot be adequately described without the introduction of a large $\langle r^4\rangle\beta_4{}^4$ parameter. In fact, it is this parameter which is responsible for the major position of the 170 cm^{-1} splitting between the levels at 1031 and 1201 cm^{-1} in $^7F_2$ as seen from equations (2) and (3).

Comparison of the emission spectra and ligand-field parameters obtained for the unsubstituted and the *p*-bromo-substituted chelates clearly indicates that the point-group symmetry of the oxygens has been drastically altered. The best agreement between experiment and theory for the di-*p*-bromo-ketoenolate is offered by model antiprism (IV). It is highly satisfactory and more than coincidental that the Eu–O distances and the angle to two ketoenolate oxygens in one ring were found to be essentially the same as those obtained for EuD_4T in the antiprism (III) configuration. These quantities are not expected to change significantly on *p*-bromo-substitution.

Model (IV) cannot explain the small values of the $\langle r^2\rangle\beta_2{}^2$ and $\langle r^4\rangle\beta_4{}^2$ which are responsible for the extremely fine splittings between the nearly degenerate levels of $^7F_1$ and $^7F_2$ (see Figure 1) since the model predicts that these parameters should be zero. However, it must be remembered that in adopting these idealized models we have ignored the steric and electrostatic effects of the associated cation,[3] and the slight inequivalence of the oxygens always found in *X*-ray data on crystalline β-ketoenolates,[9,11] and the crystal symmetry which is certainly lower than the nearest-neighbour symmetry discussed here. Any one or all these secondary effects could be responsible for the extremely fine splittings between the nearly degenerate levels.*

The value of the equivalent point charge q was estimated from expression (14) with the result †

$$\langle r^2\rangle\beta_2{}^0 = -|e|\frac{4\pi}{5}\frac{q}{R^3}\left(\frac{5}{16\pi}\right)8\,(3\cos^2\theta - 1)\langle r^2\rangle \quad (14)$$

$q = -2{\cdot}2|e|$. This, compared with the value $-1{\cdot}5|e|$ obtained for EuD_4T, suggests the possibility that *p*-bromo-substitution increases the electron density in the Eu–O bonds. Actually this is consistent with other evidence indicating that resonance effects prevail over inductive effects of substituted halogen atoms in aromatic nuclei.

This work was supported by the Atomic Energy Commission.

[1/033 *Received*, 11*th January*, 1971]

* It was shown [1] that angular displacements of the oxygen atoms of only 14′ are sufficient to produce $\langle r^2\rangle\beta_2{}^2$ and $\langle r^4\rangle\beta_4{}^2$ parameters of the magnitude reported here. Similarly, a difference in radial distance between two non-equivalent oxygens of only 0·03 Å could result in the same parameter magnitudes. This great sensitivity of these parameters to details of the ligand field is responsible for the insensitivity of the calculated bond angles and radial distances to possible small errors in the experimental determination of the ligand-field parameters when the calculation is carried out from the opposite direction.

† It is natural to obtain an equivalent point charge greater than $-0{\cdot}5|e|$ needed for electrical neutrality since the electrostatic model used does not reflect the covalent nature of the Eu–O bond which implies the presence of negative charge between the europium and oxygen atoms.